Review of Sulfuric Acid Decomposition Processes for Sulfur-Based Thermochemical Hydrogen Production Cycles

Authors:

Claudio Corgnale, Maximilian B. Gorensek, William A. Summers

Date Submitted: 2021-05-17

Keywords: hydrogen production, thermochemical processes, high temperature sulfuric acid decomposition, reactor concepts, sulfuric acid decomposition catalysts, sulfuric acid concentration

Abstract:

Thermochemical processes based on sulfur compounds are among the most developed systems to produce hydrogen through water splitting. Due to their operating conditions, sulfur cycles are suited to be coupled with either nuclear or solar plants for renewable hydrogen production. A critical review of the most promising sulfur cycles, namely the Hybrid Sulfur, the Sulfur Iodine, the Sulfur Bromine and the Sulfur Ammonia processes, is given, including the work being performed for each cycle and discussing their maturity and performance for nuclear and solar applications. Each sulfur-based process is comprised of a sulfuric acid thermal section, where sulfuric acid is concentrated and decomposed to sulfur dioxide, water and oxygen, which is then separated from the other products and extracted. A critical review of the main solutions adopted for the H2SO4 thermal section, including reactor configurations, catalytic formulations, constitutive materials and chemical process configurations, is presented.

Record Type: Published Article

Submitted To: LAPSE (Living Archive for Process Systems Engineering)

Citation (overall record, always the latest version):	LAPSE:2021.0383
Citation (this specific file, latest version):	LAPSE:2021.0383-1
Citation (this specific file, this version):	LAPSE:2021.0383-1v1

DOI of Published Version: https://doi.org/10.3390/pr8111383

processes

MDPI

Review

Review of Sulfuric Acid Decomposition Processes for Sulfur-Based Thermochemical Hydrogen Production Cycles

Claudio Corgnale [1,*], Maximilian B. Gorensek [2] and William A. Summers [1]

[1] Greenway Energy, LLC, 301 Gateway Drive, Aiken, SC 29803, USA; bill.summers@greenway-energy.com
[2] Savannah River National Laboratory, Aiken, SC 29808, USA; maximilian.gorensek@srnl.doe.gov
* Correspondence: claudio.corgnale@greenway-energy.com; Tel.: +1-803-617-9689

Received: 30 September 2020; Accepted: 29 October 2020; Published: 30 October 2020

Abstract: Thermochemical processes based on sulfur compounds are among the most developed systems to produce hydrogen through water splitting. Due to their operating conditions, sulfur cycles are suited to be coupled with either nuclear or solar plants for renewable hydrogen production. A critical review of the most promising sulfur cycles, namely the Hybrid Sulfur, the Sulfur Iodine, the Sulfur Bromine and the Sulfur Ammonia processes, is given, including the work being performed for each cycle and discussing their maturity and performance for nuclear and solar applications. Each sulfur-based process is comprised of a sulfuric acid thermal section, where sulfuric acid is concentrated and decomposed to sulfur dioxide, water and oxygen, which is then separated from the other products and extracted. A critical review of the main solutions adopted for the H_2SO_4 thermal section, including reactor configurations, catalytic formulations, constitutive materials and chemical process configurations, is presented.

Keywords: hydrogen production; thermochemical processes; high temperature sulfuric acid decomposition; reactor concepts; sulfuric acid decomposition catalysts; sulfuric acid concentration

1. Introduction

A large-scale hydrogen economy requires the production of hydrogen, to be used either as an energy carrier producing electric or mechanical work or as a chemical compound employed in chemical plants [1]. Hydrogen production requires external power input to break the bonds of the molecules containing the gas, such as water, fossil fuels and biomass. Adopting water-splitting processes, hydrogen and oxygen are the only products and a closed water cycle can be realized, producing water, again, in a fuel cell or in a combustion engine. However, the direct thermal decomposition of water happens only at high temperatures on the order of 4500 K, making the process impractical for large scale scenarios [2]. Current alternatives to the direct water splitting are electrolysis and indirect thermochemical splitting. Electrochemical water splitting is realized at temperatures close to room temperatures and achieves efficiencies on the order of 70%, requiring electric power inputs of approximately 50 kWh/kgH_2 [3,4]. Recent studies projected H_2 production costs on the order of 4.96–5.78 $/kg for large scale alkaline electrolysis systems installed in South Carolina (USA) [5]. High temperature steam electrolysis processes, in principle, can achieve a higher efficiency than low temperature electrolysis and are currently under investigation as a possible alternative process to be coupled with solar and nuclear power sources [6,7]. Water can also be split through heat-driven chemical reactions with recirculation of intermediate substances in the cycle [8–12]. Such processes, referred to as thermochemical hydrogen production cycles, have been attracting interest since the 1970s. The compounds, recirculating inside the process, are based on many different elements,

such as sulfur, iodine, bromine, iron, manganese, calcium, or chlorine, depending on the specific cycle. These compounds undergo reduction reactions, producing oxygen, and oxidation reactions, producing hydrogen. Comprehensive reviews of the main thermochemical cycles, used for both nuclear and solar applications, can be found in References [13,14]. The screening analyses [13] were carried out, identifying the performance of more than 100 cycles, based on selected characteristics and targets. The performance metric included the following characteristics: number of chemical reactions, number of product separation steps, number and abundance of chemical elements, corrosiveness of the process solutions, presence and flow of solid compounds, maximum temperature, availability of cycle chemistry demonstration data and availability of data demonstrating projected efficiency and costs [13]. Among the screened thermochemical processes, sulfur-based cycles, which see a thermal sulfuric acid decomposition section in common, were among the high-ranking processes [13]. Sulfur-based thermochemical cycles do not include any solid reactant movement and operate at relatively low temperatures (700–900 °C) compared with other competing processes. In addition, the main S-based cycles include two to three main reaction sections, limiting the complexity of the overall process and reducing the product separation sections. The main sulfur-based cycles, currently under investigation, are the Hybrid Sulfur (HyS) process, the Sulfur Iodine (SI) process and the Sulfur Bromine cycle. Two additional cycles have also been examined, namely the General Atomics S-cycle and the Sulfur Ammonia cycle. The General Atomics S-cycle was one of the first cycles proposed by General Atomics in 1970s [15]. However, after initial testing, the research and development work was interrupted mainly due to the presence of five main reactions as well as some critical thermodynamics and kinetics limitations [13,16]. The Sulfur Ammonia cycle, briefly discussed in Section 2, is being studied for solar applications but still requires additional fundamental development to propose a prototype demonstration with production of hydrogen and oxygen [17].

After an initial description and review of the main sulfur-based thermochemical cycles, the paper includes a critical review of the main approaches, configurations and solutions adopted for the H_2SO_4 thermal section, including the H_2SO_4 high temperature decomposition section, the H_2SO_4 concentration section and the SO_2-O_2 separation section. The maturity of each sulfur-based cycle, as well as the techno-economic performance achieved for nuclear and solar applications, is discussed.

2. Sulfur-Based Thermochemical Cycles

Among the thermochemical cycles being currently examined for nuclear and solar hydrogen production, sulfur-based processes are likely the most advanced systems with high potential for low-cost and high-efficiency large scale H_2 production. They are characterized by many appealing features, when compared with other thermochemical processes [13,18]. Mainly, sulfur-based cycles operate at relatively low temperatures and do not require any solid material movement. Sulfur-based processes share a high temperature sulfuric acid decomposition section, which will be described in detail in Section 3.

2.1. Main Sulfur-Based Thermochemical Cycles

2.1.1. Hybrid Sulfur Cycle

The Hybrid Sulfur (HyS) cycle was conceived by Los Alamos National Laboratory and Westinghouse [19,20]. Currently, it is one of the main cycles (and the main sulfur-based cycle) under investigation internationally for large-scale hydrogen production. Given the operating conditions, the process can be coupled with both nuclear source and concentrating solar source.

The process splits the water molecule through the recirculation of compounds based on sulfur, oxygen and hydrogen within two main chemical sections:

$$H_2SO_4 \rightarrow SO_2 + H_2O + \frac{1}{2} O_2 \quad (1)$$

$$SO_2 + 2\,H_2O \rightarrow H_2SO_4 + H_2 \quad (2)$$

The thermal decomposition of H_2SO_4 to SO_2, H_2O and O_2 (Reaction (1)) is an endothermic process, common to each sulfur-based thermochemical cycle. After the decomposition of the sulfuric acid, sulfur dioxide and oxygen are separated at lower temperatures. Sulfur dioxide is recirculated within the thermochemical process to drive the electrochemical low temperature step (Reaction (2)), while oxygen is extracted from the cycle. Hydrogen is produced in the exothermic process (Reaction (2)), through the electrochemical oxidation of SO_2. The sulfuric acid is recirculated and concentrated to drive the H_2SO_4 thermal decomposition section. The hydrogen is separated from the other products, purified and extracted from the plant.

The electrochemical section, which is the distinguishing section of the HyS process, realizes the SO_2 oxidation at an electrolyzer anode to form H_2SO_4 and hydrogen ions (H^+), which recombine with electrons and form the hydrogen molecule at the cathode. The electrolyzer works between room temperatures and about 140 °C, mainly depending on the membrane employed in the component.

The electrochemical component is currently designed either as a liquid-fed or as a vapor-fed electrolyzer. The liquid-fed configuration was developed at the Savannah River National Laboratory (SRNL), during the U.S. Department of Energy (DOE) Nuclear Hydrogen Initiative [21]. The feeding mixture (liquid SO_2 and H_2O) is oxidized at the anode of the electrolyzer to form H_2SO_4, which feeds the thermal decomposition section, H^+ protons and electrons. Protons pass through the electrolyzer membrane to the cathode and recombine with external electrons to form H_2 [22–24]. One of the main issues associated with the use of the liquid fed electrolysis system approach was the sulfur dioxide cross over through the component membrane. Recent experimental data, collected at the SRNL, demonstrated the ability of a novel configuration employing proton exchange membrane (PEM) to prevent sulfur accumulation and sulfur dioxide crossover [25]. The vapor fed electrolysis configuration has recently been developed at University of South Carolina and SRNL [26]. Dry vapor SO_2 is fed to the anode of the electrolyzer, while liquid H_2O is fed to the cathode of the component. Water diffuses across the membrane to the anode because of the water activity difference and pressure gradients. Water is also transported again to the electrolyzer cathode by electro-osmotic drag. Sulfuric acid and hydrogen protons are produced at the anode. The protons then recombine with electrons to produce hydrogen at the cathode of the component [26].

The reversible cell potential of the electrochemical SO_2 oxidation reaction is 0.158 V, i.e., approximately 13% of the water electrolysis potential (1.229 V). The electrolyzer is currently designed adopting a traditional PEM fuel cell approach, allowing a compact design, reduced footprints and lower cost solutions [23,24]. Recent work demonstrated that a PEM electrolyzer, employing sulfonated polybenzimidazole (s-PBI) membranes, has high potential to achieve a practical cell potential of 0.6–0.7 V at current densities on the order of 500 mA/cm^2 [27–29] This cell potential value is equal to approximately one third of the actual water electrolysis potential (i.e., 1.8 V) [20,30]. Platinum material has been adopted as the baseline catalytic formulation to reduce the kinetics overpotential of the SO_2 oxidation reaction [31]. However, recent in-situ tests showed that Au nanoparticle catalysts seem to exhibit high current densities and greater stability than Pt nanoparticle catalysts [32].

The electric input, mainly required to operate the electrochemical oxidation of the sulfur dioxide, represents approximately 20% of the thermochemical process input [22]. The thermochemical process efficiency has been assessed to be equal to (realistic) values on the order of 30–40% (based on the hydrogen LHV), depending on the process flowsheet, the layout and on the electric power generation efficiency [30,33–35]. Techno-economic analyses, carried out for both nuclear driven and solar driven HyS processes, identified realistic nuclear H_2 production costs on the order of 5.34–6.18 $/kg [36]. Reduced costs could be achieved only with high efficiency HyS process configurations and operating with high temperature nuclear reactors [37]. Solar-driven HyS processes were examined and developed for coupling with concentrating solar power plants. Hydrogen production costs were assessed to be on the order of 2.64–7.58 $/kg depending on the characteristics of the solar plant (e.g., thermochemical efficiency, heliostat cost, solar plant efficiency, location) [22,34,38,39]. Selected solar

HyS plant configurations demonstrated potential to produce hydrogen at costs that can closely approach the DOE target of 2 $/kg. [40].

2.1.2. Sulfur Iodine Cycle

The Sulfur Iodine (SI) cycle was originally developed by General Atomics [13,16,41], mainly focusing on nuclear power applications.

The SI cycle has three main sections, based on compounds of sulfur, iodine, hydrogen and oxygen:

$$H_2SO_4 \rightarrow SO_2 + H_2O + \frac{1}{2} O_2$$

$$2\,HI \rightarrow I_2 + H_2 \quad (3)$$

$$I_2 + SO_2 + 2\,H_2O \rightarrow H_2SO_4 + 2\,HI \quad (4)$$

The thermal decomposition of H_2SO_4 into SO_2, H_2O and O_2 (Reaction (1)) produces sulfur dioxide and water and oxygen. Sulfur dioxide and oxygen are recycled in an exothermic section (Reaction (4)), referred to as the "Bunsen" section, while oxygen is separated from the other compounds and extracted from the plant as byproduct. Hydrogen is produced in Reaction (3), which is the distinguishing SI plant section, where hydrogen iodide (HI) decomposition to hydrogen and iodine takes place. An aqueous hydrogen iodide mixture, feeding the section at relatively low HI concentrations, requires HI concentration to operate an effective and low energy HI decomposition. The HI section is a critical step in the SI process, due to the homogeneous azeotrope in the system HI-H_2O making the acid concentration and decomposition highly energy intensive and expensive [42]. Three methods have mainly been examined to concentrate and decompose the hydrogen iodide: the extractive distillation, the membrane-based distillation (i.e., electro-electrodialysis distillation) and the reactive distillation [43–45]. The extractive distillation concept was examined by General Atomics, proposing the I_2 separation by extractive distillation using H_3PO_4 [41,46]. However, this approach essentially adds another compound (i.e., another section) to the cycle, requiring additional separation units, reactors and electric power input to recycle the phosphoric acid [47]. The electrodialysis distillation approach was proposed by Japan Atomic Energy Agency and Korea Institute of Energy Research [47], but still requires fundamental development for a prototype level demonstration [45,48]. The reactive distillation column approach, proposed by Knoche et al. [49], allows the separation of HI from the other compounds and the decomposition of the hydrogen iodide in a single column. This occurs by utilizing the pressure shift of azeotropic and quasi-azeotropic composition [50]. The reactive distillation approach shows some techno-economic hurdles to be overcome: (1) the column reboiler requires critical high temperature thermal power supply, which is currently provided through a heat pump that increases the plant investment cost and the lifetime costs due to the additional electric input and (2) fundamental research is still required to fully understand the reaction thermodynamics and kinetics [42,44].

The product of the HI section, after hydrogen separation, is recirculated in the Bunsen section, reacting with the H_2SO_4 section product, to produce sulfuric acid and hydrogen iodide and close the overall cycle. The Bunsen reaction is exothermic and occurs at temperatures on the order of 100–120 °C [13,51]. Additional work is required to demonstrate the Bunsen reaction, as well as the overall SI cycle, at a prototype level.

Realistic thermochemical efficiencies of 35–38% (based on H_2 LHV) were assessed [44,52], also showing high sensitivity to the HI decomposition process configuration [42,47]. The nuclear hydrogen production cost was estimated to be on the order of 3.50–12.0 $/kg depending on the SI cycle and the nuclear reactor configuration [42,52].

2.1.3. Sulfur Bromine Cycle

The Sulfur Bromine cycle was originally developed at the Ispra facilities during the 1970s [43,53].

The cycle has three main sections, based on sulfur, bromine, hydrogen and oxygen compounds:

$$H_2SO_4 \rightarrow SO_2 + H_2O + \frac{1}{2} O_2$$

$$2\ HBr \rightarrow Br_2 + H_2 \quad (5)$$

$$Br_2 + SO_2 + 2\ H_2O \rightarrow H_2SO_4 + 2\ HBr \quad (6)$$

Similarly to the other sulfur cycles, the high temperature decomposition of sulfuric acid (Reaction (1)) produces oxygen and sulfur dioxide. The distinguishing section is the electrochemical decomposition of HBr (Reaction (5)), producing hydrogen, separated from the other compounds and extracted from the process, and bromine. The hydrogen bromide is decomposed to bromine and hydrogen at temperatures in the range of 80–200 °C depending on the electrolyzer characteristics [43]. The electrolysis unit was developed and tested during the 1970s and 1980s, showing voltages on the order of 0.8–1.0 V at current densities of approximately 100–600 mA/cm^2 [54]. The exothermic recombination of Br and SO_2 (Reaction (6)) occurs at temperatures in the range of 20–100 °C.

The cycle was tested producing hydrogen at 100 LH_2/h for 150 h, with thermochemical process efficiencies on the order of 37% [43]. Currently, the cycle is not under investigation for nuclear or solar applications, mainly due to the high voltage required in the electrolysis unit.

2.1.4. Sulfur Ammonia Cycle

The Sulfur Ammonia process was recently conceived by the Florida Solar Energy Center for solar applications [55]. The cycle represents an attempt to use both the thermal and the photonic components of the solar input. The cycle is comprised of five main reactions, based on sulfur, nitrogen, potassium, hydrogen and oxygen compounds, and requires a suitable solar system to collect both the thermal input and the solar light input:

$$SO_2 + 2NH_3 + H_2O \rightarrow (NH_4)_2SO_3 \quad (7)$$

$$(NH_4)_2SO_3 + H_2O \rightarrow (NH_4)_2SO_4 + H_2 \quad (8)$$

$$(NH_4)_2SO_4 + K_2SO_4 \rightarrow K_2S_2O_7 + 2NH_3 + H_2O \quad (9)$$

$$K_2S_2O_7 \rightarrow K_2SO_4 + SO_3 \quad (10)$$

$$SO_3 \rightarrow SO_2 + \frac{1}{2} O_2 \quad (11)$$

The cycle distinguishing reaction (Reaction (8)) is the photocatalytic production of hydrogen and ammonium sulfate from an aqueous ammonium sulfite solution, occurring above room temperature (approximately 80–150 °C) and low pressures [56,57]. A sub-cycle is identified by the Reaction (9) and Reaction (10). Ammonium sulfate product is reacted with potassium sulfate (Reaction (9)), at temperature on the order of 400 °C, to generate potassium pyrosulfate, which is decomposed (Reaction (10)) at temperatures on the order of 550 °C, to K_2SO_4 and SO_3 [57]. K_2SO_4 is recirculated to drive Reaction (9) and close the sub-cycle. SO_3 is catalytically decomposed to SO_2 and O_2 (Reaction (11)), as for the other sulfur-based thermochemical processes, at high temperatures on the order of 800–1000 °C. The separation of sulfur dioxide and oxygen occurs in Reaction (7) with water mixing and production of aqueous ammonium sulfite. Thermodynamic and kinetics tests demonstrated the feasibility of the proposed cycle at laboratory scale [56], but additional work is required to demonstrate the actual performance of a closed cycle at prototype level.

3. Sulfuric Acid Thermal Decomposition

Every sulfur-based thermochemical cycle is comprised of a high temperature section, referred to as H_2SO_4 thermal section, where sulfuric acid is decomposed to sulfur dioxide, oxygen and water.

The sulfur dioxide and the water are separated from the oxygen, which is extracted from the cycle as byproduct, and processed in the other sections of the thermochemical cycles. The main processes occurring in the H_2SO_4 thermal section are: (1) high temperature decomposition of concentrated sulfuric acid, (2) concentration of the inlet sulfuric acid mixture, (3) separation of the oxygen from the sulfur dioxide mixture. The oxygen is then purified, reaching the required purity targets, and extracted from the plant as byproduct.

3.1. High Temperature Sulfuric Acid Decomposition

The sulfuric acid decomposition section is the highest temperature section of each sulfur-based thermochemical process, where the endothermic decomposition of H_2SO_4 to SO_2, H_2O and O_2 occurs. The H_2SO_4 decomposition takes place in two separate steps. The first reaction sees the vaporization and the instantaneous (i.e., equilibrium) decomposition of the H_2SO_4 mixture, feeding the section, to SO_3 and H_2O, as shown in Reaction (12), at temperatures in the range of 300–450 °C:

$$H_2SO_4 \rightarrow SO_3 + H_2O \quad (12)$$

The second reaction sees the decomposition of the products of Equation (12) to SO_2 and O_2, as shown in Equation (13):

$$SO_3 + H_2O \rightarrow SO_2 + H_2O + \frac{1}{2} O_2 \quad (13)$$

The endothermic reaction of Equation (13) is thermodynamically favored at high temperatures and low pressures. For a reasonable conversion, this reaction should take place at temperatures usually on the order of 750–900 °C. The feeding sulfuric acid mixture is at temperatures of approximately 200–300 °C and concentrations on the order of 70–90 wt %, depending on the plant configuration and the operating conditions. Figure 1 shows the equilibrium SO_2 conversion of a sulfuric acid solution at 90 wt % at temperatures between 500 °C and 900 °C and pressures between 1 bar and 50 bar.

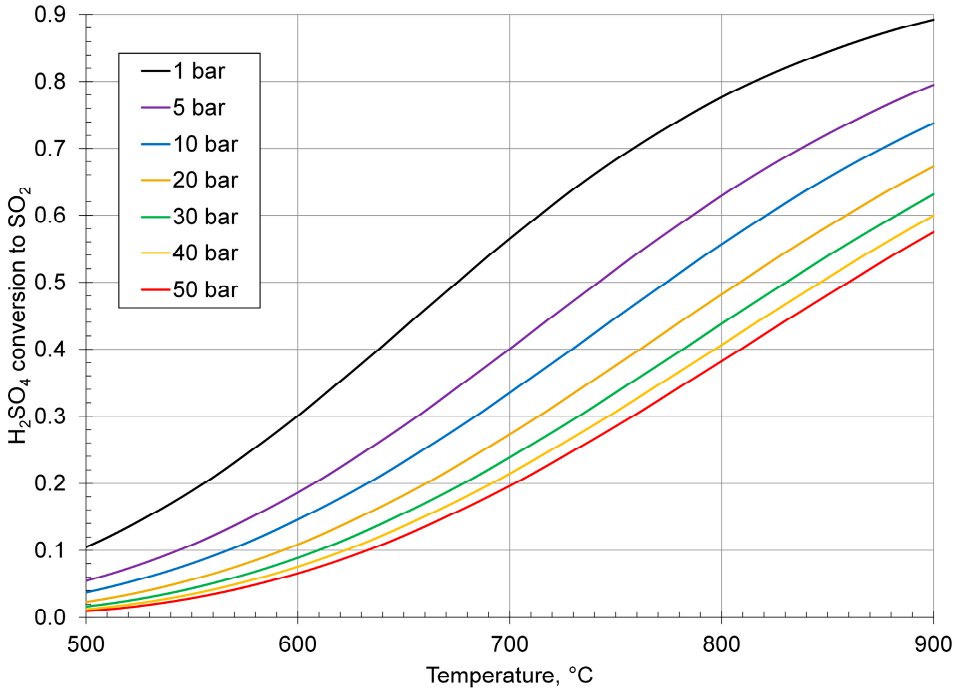

Figure 1. H_2SO_4 fractional conversion to SO_2 at equilibrium for the 500–900°C temperature and 1–50-bar pressure ranges (calculated by Gibbs free energy minimization using the symmetric Electrolyte Non-Random Two Liquid (eNRTL) model [58] for a 90-wt % H_2SO_4 solution vaporized, heated, and pressurized to the indicated conditions).

The reacted mixture is condensed and cooled to achieve the required conditions to separate oxygen. The undecomposed SO_3 reacts with water to produce H_2SO_4 again, following the reaction in Equation (12). The thermal power available from the cooling, condensation and exothermic formation of H_2SO_4 can be internally recovered to drive the H_2SO_4 decomposition reaction.

The main challenges faced with the development of an effective sulfuric acid decomposition process are mainly related to: (1) identification of suitable constitutive materials, being able to withstand aggressive and high temperature environments, (2) identification of high performance catalytic materials, to achieve high activity, reduced degradation and suitable costs for large scale hydrogen production and (3) identification of effective heat transfer configurations, allowing both an effective external source heat exchange and a proper internal heat recovery.

3.1.1. Constitutive Materials

Several comprehensive tests were carried out during the DOE Nuclear Hydrogen Initiative, examining the behavior of different (i.e., ceramic and metallic) constitutive materials. The performance was measured under selected conditions and configurations, including different sulfuric acid concentrations, temperatures and structural configurations [59,60]. Ceramic materials, namely SiC, were found to be the most (and likely only) suitable materials for the high temperature sulfuric acid vaporization and decomposition, given the operating temperatures and the aggressive environment [59,60]. Table 1 [59] summarizes the corrosion test results obtained for concentrated sulfuric acid vaporization and decomposition at 1 bar under different temperature ranges.

Table 1. Summary of material options for the sulfuric acid decomposition process [59]. (Reproduced with permission from General Atomics).

Process	Conditions	Candidate Materials	Compatibility–Corrosion Results	Comments
H_2SO_4 vaporization	350–550 °C $H_2O + SO_3$, other contaminants	Structural: Incoloy 800 H AL610, high Si steel SiC, Si_3N_4 Hastelloy G, C-276	800 H, 800 HT. High Si steel (SiO_2) < 5 mm/year. SiC ≈ no corrosion in 1000 h test at 75–79% acid. C-276 ≈ 1 mm/year at 476 h.	Coated materials (Pt) cost issue. Ceramics promising, but fabrication and joining issues. Dry wall boiler with ceramics may be an option.
H_2SO_4 decomposition	550–950 °C H_2O, H_2SO_4, SO_3, SO_2, O_2	Structural: Incoloy 800 HT, Incoloy 800 H (with aluminide coatings), AL610 Ceramics, Pt or Au coatings on superalloy structural materials	Incoloy, Inconel bare–2–4 mg/cm^2 in 1000 h at 900 °C. Aluminide coatings—approximately 1 mg/cm^2 in 1000 h at 900 °C. Intergranular corrosion observed for 800 H. Noble metal coatings may provide corrosion protection.	Incoloy 800 HT may address integranular corrosion. C-SiC composites should be examined. Pt coatings may serve the function of catalyst and reduce corrosion. Corrosion benefits of noble metal coatings must be demonstrated.

A more recent work, carried out in Japan, also examined the performance of constitutive materials in high temperature sulfuric acid mixtures for thermochemical hydrogen production cycles [61]. The authors examined similar candidate materials as those shown in Table 1. For lower temperature operations (i.e., vaporization) the main candidates were: SiC, Si_3N_4, FeSi (i.e., high silicon iron materials) and Au, while for the high temperature gas decomposition the main candidates were: Incoloy 800, Hastelloy C276, Inconel 625 and SiC. Corrosion tests were conducted at H_2SO_4 concentrations of 75 wt %, 85 wt % and 95 wt %, temperatures of 320 °C, 380 °C and 460 °C, pressures up to 20 bar and exposures up to 1000 h. The corrosion rates, measured for all SiC, Si-SiC (SiC at 80 wt % and Si at 20 wt %) and Si_3N_4 specimens, showed excellent resistance with absence of weight changes [61]. FeSi materials with silicon content of 20 wt % showed evidence of crack formation [61].

Recent work, carried out as part of the European Union funded HycycleS project, examined the behavior of several materials, i.e., alumina, tantalum-coated steel and materials from the SiC-family, analyzing their stability in concentrated sulfuric acid vaporization and decomposition processes by carrying out long-term corrosion tests [62,63]. Post-characterization of the materials revealed that Siliconized SiC (Si-SiC) was the most suitable material for sulfuric acid vaporization and decomposition [62].

3.1.2. Catalysts

A comprehensive list of catalytic materials, used for the H_2SO_4 decomposition process during the initial development of sulfur-based thermochemical hydrogen production cycles, can be found in the studies carried out in the USA (by General Atomics and Westinghouse) and in Japan (by Yokohama National University) in the late 1970s and 1980s [16,20,51,64,65]. Table 2 summarizes the test results carried out at General Atomics [51].

Table 2. Studies of various catalysts for H_2SO_4 decomposition (≈0.5 s residence time) [51] (Reproduced with permission form General Atomics).

Catalyst	Onset of Failure Temperature (K)	Failure Mode
0.5% Pt/Al_2O_3	890	$Al_2(SO_4)_3$ poisoning
Fe_2O_3/Al_2O_3	1000	Sulfate formation
V_2O_5/Al_2O_3	910	Sulfate formation, volatile
Cr_2O_3/Al_2O_3	1070	Sulfate formation, volatile
CuO/Al_2O_3	950	Sulfate formation
0.1% Pd/Al_2O_3	970	$Al_2(SO_4)_3$ poisoning
MnO_2/Al_2O_3	1120	Sulfate formation
CoO/Al_2O_3	1140	Sulfate formation
NiO/Al_2O_3	1160	Sulfate formation
0.1% Pt/Al_2O_3	950	$Al_2(SO_4)_3$ poisoning
Al_2O_3	1250	Poor catalyst
CuO/SiO_2	1010	$CuSiO_3$ formation?
0.5% Pt/SiO_2	850	Gradual temperature cut-off
CeO_2	1180	Poor catalyst
0.08% Pt/TiO_2 (surface)	800	Gradual temperature cut-off
0.1 % Pt/TiO_2	900	Gradual temperature cut-off
Pd/TiO_2	1090	Initially better, sulfation?
Fe_2O_3/TiO_2	1090	Unknown
CuO/TiO_2	1000	Sulfate formation
0.08% Pt/TiO_2	790	Gradual temperature cut-off
TiO_2	1140	Poor catalyst
Pt/ZrO_2 (surface)	830	Substrate sulfation
Fe_2O_3/ZrO_2	1020	Sulfate formation
CuO/ZrO_2	970	Sulfate formation
ZrO_2	1130	Poor catalyst

Table 2. *Cont.*

Catalyst	Onset of Failure Temperature (K)	Failure Mode
$Nb_2O_5/BaSO_4$	1140	Poor catalyst
$CuO/BaSO_4$	1050	Sulfate formation
$Fe_2O_3/BaSO_4$	980	Sulfate formation
$U_3O_8/BaSQ_4$	1070	Sulfate formation
$BaSO_4$	1250	Poor catalyst
0.07% $Pt/BaSO_4$-TiO_2	780	Gradual temperature cut-off

The main conclusions of the study described in ref. [51] are indicated here below. Some metals, such as chromium, nickel, manganese, cerium and uranium, failed to achieve acceptable catalytic activity, mainly due to formation of stable sulfates at relatively high temperatures. Results relative to the substrates showed that Al_2O_3 is a poor substrate for platinum group metals, probably due to the platinum catalysts poisoning by $Al_2(SO_4)_3$. Catalyst vaporization was also demonstrated to be another reason of poor performance. A few catalysts (e.g., V_2O_5, Cr_2O_3) seemed to move downstream and coat colder walls, acting as a reverse catalyst [51]. For systems operating at high temperatures and low pressures, oxide materials (e.g., Fe_2O_3 and CuO) seemed to show good performance. The authors concluded that the following catalysts: $Pt/BaSO_4$-TiO_2, Pt/TiO_2, Pt/ZrO_2, and Pt/SiO_2 were found to be suitable systems at a large range of temperatures [51].

Following the outcomes from the initial catalytic material work, more recent activities (in the 2000s), funded by the DOE as part of the Nuclear Hydrogen Initiative [66], focused on identifying the performance of Pt catalysts on different supports. Idaho National Laboratory was the leading institution for H_2SO_4 decomposition catalyst development in the Nuclear Hydrogen Initiative, examining activity and degradation of Pt catalysts with different supports [67,68]. Results showed the feasibility of selected Pt formulations on TiO_2 support with reduced deactivation after an initial activity decrease. In the studies carried out by Idaho National Laboratory [68], samples of 1 wt % Pt/TiO_2 (rutile) catalysts were exposed to sulfuric acid mixtures flowing at 1123 K and 1 bar for times on stream between 0 and 548 h (Figure 2).

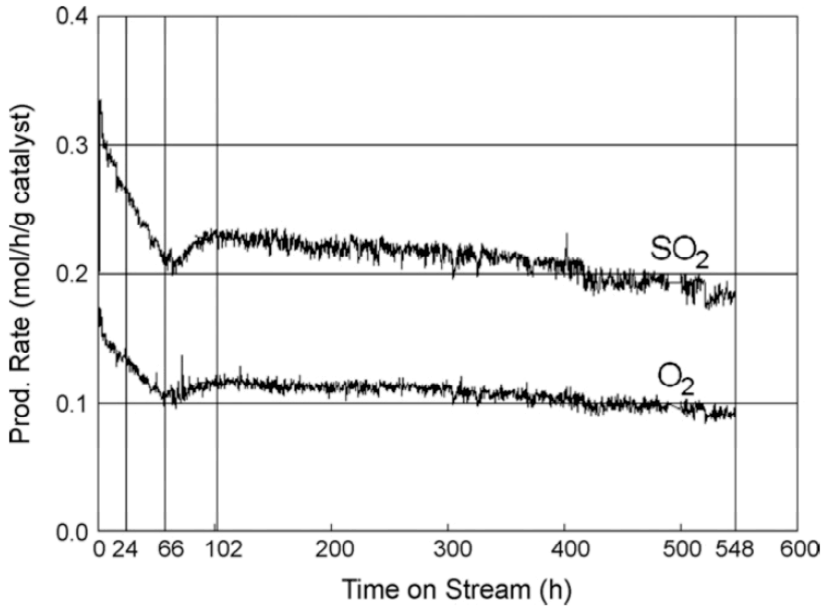

Figure 2. SO_2 and O_2 production rates as a function of time on stream (H_2SO_4 concentration 95.7 wt %, pressure 1 bar, measured temperature 1113 ± 10 K) [68]. (Reproduced with permission from Ginosar D, Applied Catalysis A: General, 2008).

Pt sintering and oxidation were likely the main issues observed under the adopted conditions and some Pt was lost by volatilization. Results showed an initial catalyst activity reduction (about 66 h), with a subsequent recovery (up to approximately 102 h). A slow deactivation period, between 102 h and the end of the testing time on stream, was observed. Catalyst sulfation did not seem to be detrimental to catalyst activity and the activity profile seems to highlight a complex dynamical situation, including platinum sintering, oxidation, and sublimation, along with TiO_2 morphological changes, that affected the catalyst activity [68]. The sulfation of the Pt catalyst did not seem to be the reason for the performance reduction.

Alternatives to the Pt/TiO_2 catalyst are currently being investigated to find a catalytic formulation with long stability and reduced deactivation. One of the options is to use metal oxides in different configurations. Idaho National Laboratory also examined the behavior of complex metal oxides analyzing the performance for accelerated stability testing (about 160 h) at 850 °C and atmospheric pressure [69]. The following metal oxides were analyzed: $FeTiO_3$, $MnTiO_3$, $NiFe_2O_4$, $CuFe_2O_4$, $NiCr_2O_4$, $2CuO{\cdot}Cr_2O_3$, CuO, Fe_2O_3. The authors stated that every material examined in the study displayed shortcomings including material sintering, phase changes, low activity at moderated temperatures due to sulfate formation and decomposition to their individual oxides. The final statement from the authors on metal oxide catalysts was that more effort would be needed to discover metal oxide materials that are less expensive, more active and more stable than platinum catalysts [69]. A more recent work, carried out by a European consortium (HycycleS), also investigated the possibility of using metal oxides in different configuration and rector structures [62,70,71]. The authors carried out a comparative assessment of Fe_2O_3, CuO, Cu–Fe, Fe–Cr, Cu–Al and Cu–Fe–Al mixed oxides coated as catalysts on silicon carbide monolithic honeycomb structures, with respect to sulfuric acid decomposition reaction conditions for 100 h at 850 °C and ambient pressure [62]. The study concluded that Fe_2O_3, CuO and Fe–Cr mixed oxide retained their chemical and structural stability after exposure to reaction conditions, while the other three mixed oxides studied suffered from significant phase decomposition phenomena [62]. In general, every study about metal oxides concluded that selected formulations may be considered as a promising alternative to Pt-based catalytic formulations with potential for high catalytic activity and high stability. However, additional investigation is required for a commercial use of metal oxide catalysts, especially to avoid sintering phenomena and catalytic activity reduction experienced at temperatures lower than 800 °C, as shown in Figure 3 [69].

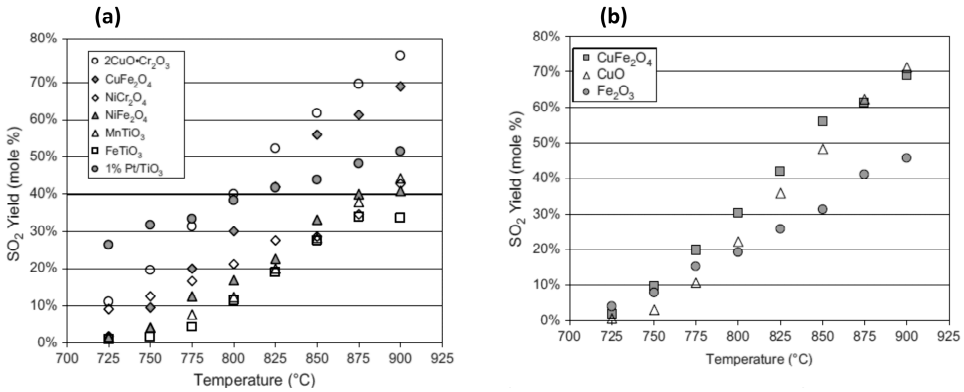

Figure 3. Temperature dependent SO_2 yields over metal oxide materials: (**a**) complex metal oxides; (**b**) copper and iron simple and complex metal oxides) between 725 and 900 °C at 1 bar and a weight hour space velocity (WHSV) of approximately 50 g acid/g catalyst/h [69]. (Reproduced with permission from Ginosar D, Int J Hydrogen Energy, 2009).

Another catalytic formulation, alternative to the single metal Pt/TiO_2 catalyst, sees the use of bimetallic catalytic materials on different supports. This is a novel concept for the H_2SO_4 decomposition reaction and recent research and development activities have been carried out by Idaho National Laboratory, the University of South Carolina and Greenway Energy, as part of the DOE Hydrogen

and Fuel cells Technology Office (HFTO) HydroGEN consortium [72]. Initial results demonstrated the ability of the a Pt/Ir formulation on boron nitrite (BN) support (namely 1wt %Pt/7.5wt %Ir/BN) to achieve high activities and essentially absence of degradation for about 75 h under a 91 wt % H_2SO_4 concentrated flow at 800 °C and 1 bar [72]. Additional testing will be required for longer duration performance assessment.

3.1.3. Reactor Concepts

Two main approaches are currently being investigated to identify effective high temperature H_2SO_4 decomposition reactor configurations. The first reactor concept, which sees a direct coupling of the H_2SO_4 decomposition process with the external thermal source, is referred to as a direct cavity reactor, and is especially suited for solar applications. The second concept is referred to as an indirect solar tubular reactor and is based on an indirect coupling with the external source. In the first configuration, the thermal power is provided directly by the primary source without the presence of intermediate heat exchanger loops. The second concept includes an intermediate heat transfer fluid, transferring the required thermal input and exchanging it with the H_2SO_4 mixture.

The German Aerospace Center (DLR) has been developing one of the main direct cavity reactor configurations (currently under development) with two solar absorbers in series, where the vaporization reaction and the catalytic decomposition reaction take place in separate units, as shown in Figure 4 [73,74]. This allows specific and different designs for the two separate reactions to be used.

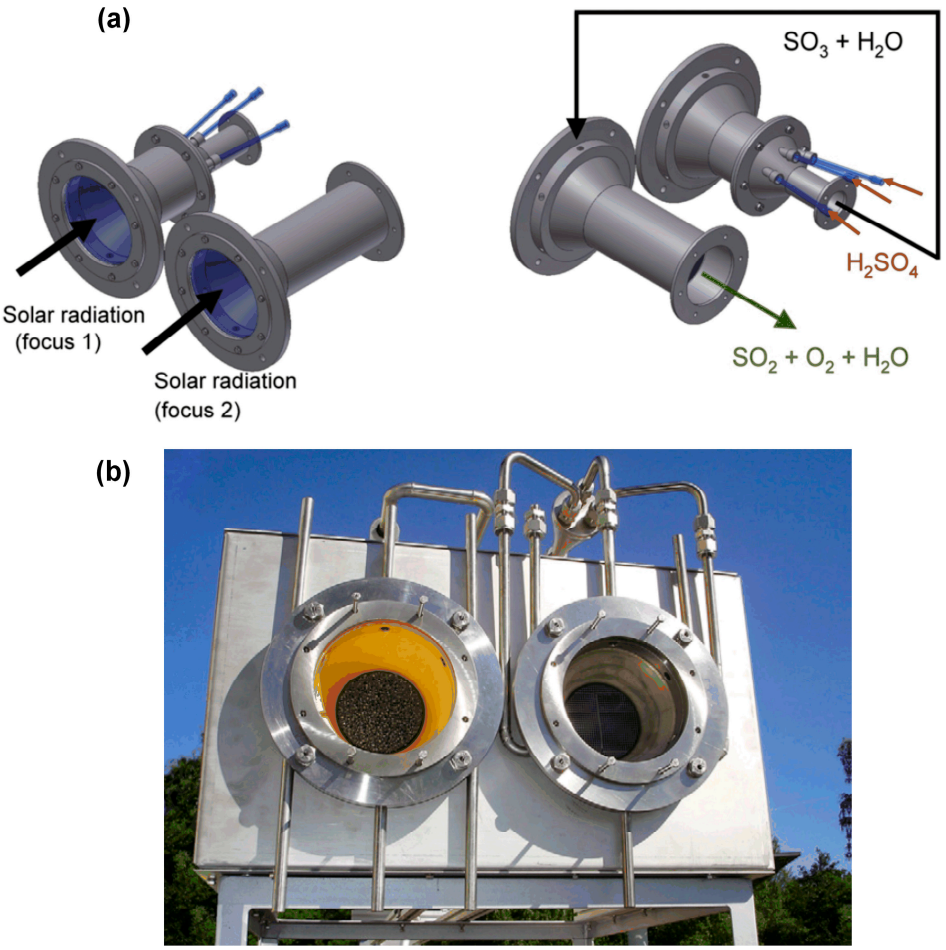

Figure 4. Two-unit direct H_2SO_4 vaporization and decomposition reactor: (**a**) conceptual design; (**b**) experimental solar driven reactor at German Aerospace Center (DLR) with foam absorber in evaporator (left) and honeycomb decomposer (right) [74]. (Reproduced with permission from Roeb M, Int J Hydrogen Energy, 2012).

A laboratory scale concept was tested at the DLR facilities. The feeding acid vaporized in a ceramic foam absorber (left side reactor in Figure 4b), which collects to the concentrated solar power through a quartz window. The intermediate products (SO_3, H_2O) flowed through the second absorber (honeycomb structure, right side reactor in Figure 4b), where the decomposition of SO_3 to SO_2 took place. The SO_3 decomposition reactor tests were carried out at atmospheric pressure and temperatures of approximately 850 °C, with peak values of 1200 °C. The reactor was also tested, examining the behavior under different H_2SO_4 concentrations and different catalytic formulations. SO_3 reaction yield close to the equilibrium values was demonstrated using Pt catalyst and operating at temperatures of 1000–1200 °C [73]. The use of metal oxide catalysts based on Fe or Cu was also successful, showing conversions of SO_3 to SO_2 of more than 80% at temperatures of approximately 850 °C [74].

The proposed direct reactor concept shows some barriers to achieve an effective internal heat recovery. Since the H_2SO_4 decomposition takes place in two separate units, a separate heat transfer unit is required to internally recover the heat available from the high temperature reacted mixture. The concept proposed by DLR also requires further development for a prototype level demonstration at pressures higher than 1 bar.

The main indirect reactor concept proposed recently for the H_2SO_4 decomposition, either using a nuclear source or a solar source, is based on a reactive bayonet heat exchanger concept. The concept was originally developed as part of the DOE Nuclear Hydrogen Initiative [75] and demonstrated at SNL at laboratory scale SO_2 productions (i.e., H_2 productions) of approximately 100 L/h [76]. A schematic is shown in Figure 5.

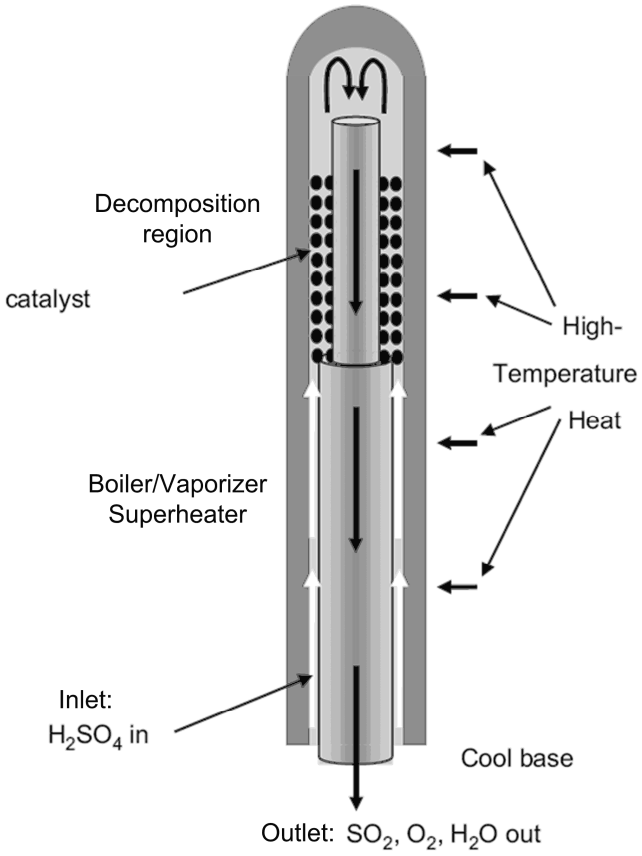

Figure 5. Indirect H_2SO_4 vaporization and decomposition bayonet heat exchanger-based reactor.

The inlet mixture (H_2SO_4 in) feeds the component at temperatures on the order of 200–300 °C through an annular region, from the inlet to the dome of the component. The concentrated H_2SO_4 is

vaporized and decomposed to SO_3 in the bottom part of the annular region, reaching temperatures of approximately 450 °C.

The SO_3 mixture is then superheated (up to 600–700 °C) before the catalytic decomposition to SO_2 in the upper region of the component occurs.

The reacted SO_2 mixture flows through the cylindrical inner region of the reactor down to the base at low temperatures. The heat required to decompose the acid is provided by an external heat transfer fluid (the "High-Temperature Heat" region in Figure 5) and the internal heat recovery from the reacted mixture flowing through the inner region.

In principle, the bayonet reactor has two main advantages over other possible configurations: (1) the heat, available from the exothermic reactions, can be internally recovered in a single unit, and (2) the reactor ceramic structure and the plant interfaced metal equipment can be connected at low temperatures (200–250 °C), avoiding any metal–ceramic material connection issues.

The reactor, initially developed for nuclear applications, was suitably adapted to be coupled with concentrating solar power plants, using helium as the intermediate heat transfer fluid [22,77].

Figure 6 shows the results of a pinch analysis applied to model the fluid vaporization and decomposition as well as the cooling and condensation with internal heat recovery in the bayonet reactor. The approach used to simulate the component is detailed in References [30,78], but modified to use the symmetric eNRTL model developed by Kaur et al. [58] for thermodynamic properties. The specific case was simulated assuming a maximum temperature of 875 °C, pressure equal to 35 bar and inlet H_2SO_4 concentration equal to 82 wt % and examining the equilibrium conditions, without including any kinetics effect. The reactive mixture (dashed line in Figure 6) goes through the following processes: (1) initial heating process (up to temperatures of approximately 400 °C), (2) vaporization and decomposition of H_2SO_4 to SO_3 (up to temperatures on the order of 500 °C), (3) superheating of the reacted mixture (up to 650 °C) and (4) high temperature decomposition of SO_3 to SO_2 (up to 875 °C). The reacted mixture (solid line in Figure 6) is cooled, reaching approximately 500 °C, with following condensation and reassociation of SO_3 to H_2SO_4 achieving a final temperature of approximately 245 °C. The heat duty from the external source (Figure 6) is 347.3 kJ/molH_2 under the operating conditions described above [72].

Additional sensitivity pinch analyses, carried out at different pressures, temperatures and acid concentrations, can be found in References [30,78].

Results obtained from CFD simulations also showed the technical feasibility of a solar driven bayonet reactor, with He as the intermediate heat transfer fluid. Temperature and concentration profiles showed the ability of the proposed concept to closely approach the equilibrium yield at temperatures of 850 °C, employing a Pt-based catalyst [79]. The adoption of a bayonet reactor in solar power applications requires the presence of an intermediate heat exchanger (i.e., using He as heat transfer fluid), resulting in additional capital costs and reduced performance of the overall plant [22].

Recently, a novel reactor concept has been proposed within the DOE HydroGEN program [80], which allows the direct external source heating and the internal heat recovery to be realized in a single unit, without any intermediate heat transfer fluid. A single unit conceptual design, driven by solar radiation, is shown in Figure 7 [80].

Results of CFD simulations carried out for the unit shown in Figure 7, with a feeding H_2SO_4 mixture of 0.28 kg/s, showed the effectiveness of the proposed concept for maximum temperatures on the order of 875 °C, inlet pressure equal to 14 bar and inlet concentration of 82 wt %. Results highlighted an effective internal heat recovery, maintaining temperature differences of less than 100 °C between the inlet (reactive) and the outlet (reacted) mixtures, and a proper SO_3 decomposition [80]. Additional optimization of the proposed concept should be carried out, to design and demonstrate a commercial-scale reactor configuration.

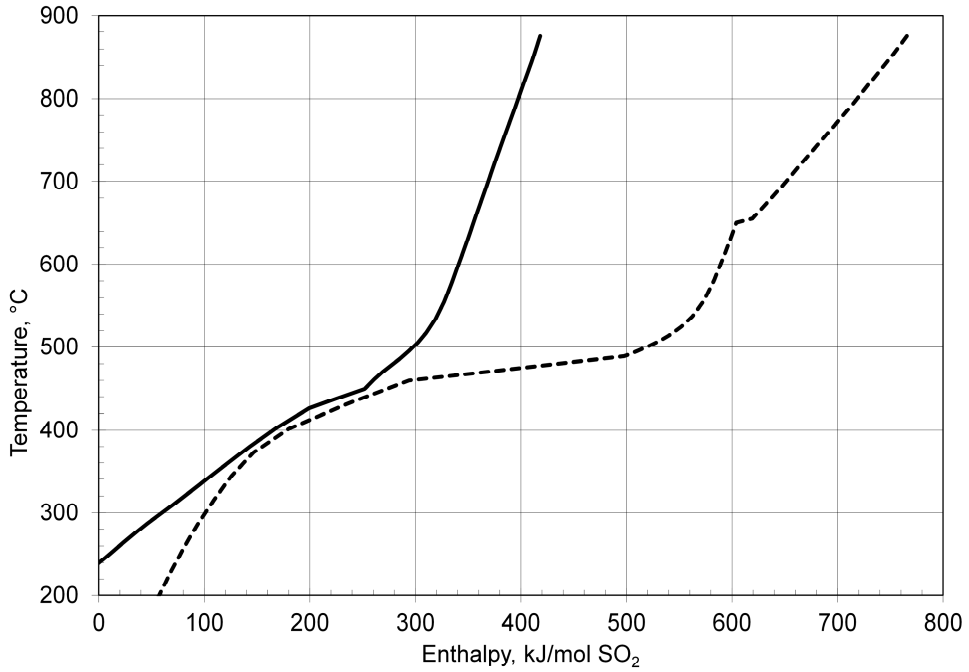

Figure 6. Pinch analysis composite curves with heating (dashed profile) and cooling (solid profile) profiles for a sulfuric acid decomposition reactor (e.g., bayonet reactor) with internal heat recovery (maximum temperature = 875 °C, pressure = 35 bar, inlet H_2SO_4 concentration = 82 wt %).

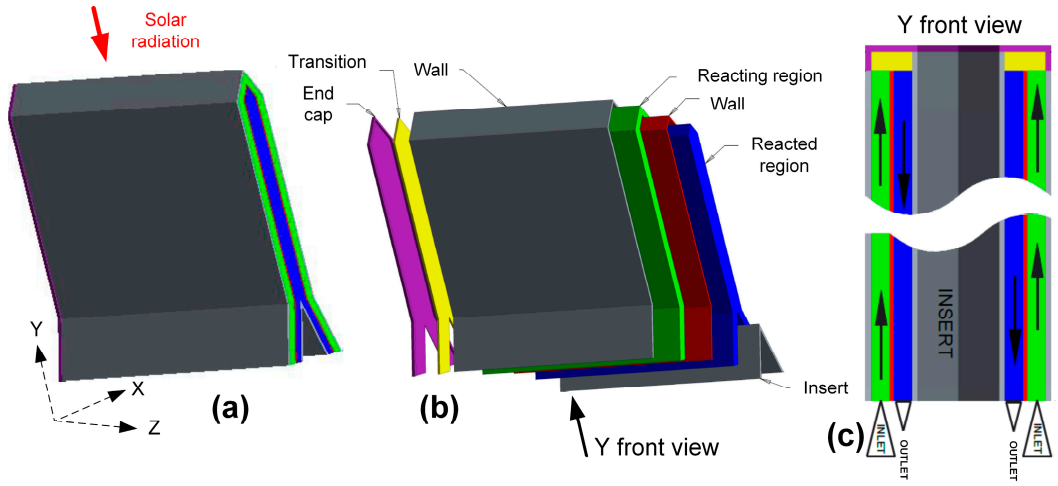

Figure 7. Direct solar receiver–reactor concept: three-dimensional view of the reactor (**a**), exploded view of the reactor (**b**) and Y axis front view of the reactor (**c**) [80]. (Reproduced with permission from Corgnale C, Int J Hydrogen Energy, 2019).

3.2. Sulfuric Acid Concentration

Sulfuric acid mixtures, produced internally in sulfur processes, need concentrating to achieve suitable H_2SO_4 concentrations to feed the high temperature decomposer. Two main, traditional approaches are used to concentrate sulfuric acid, using either low temperature and low (sub-atmospheric) pressures or higher temperatures and pressures on the order of 1–10 bar.

The first acid concentration concept uses low pressure (vacuum) distillation columns, usually operating at pressures on the order of 0.1 bar, with column reboiler temperatures on the order of 120–160 °C, depending on the required H_2SO_4 concentration, and column condenser temperatures of about 40 °C [30,35]. A single distillation column is generally adequate for typical operating conditions

of sulfur thermochemical cycles, where an H_2SO_4 concentration in the range of 75–90 wt % is required to achieve suitable efficiencies in the high temperature H_2SO_4 decomposition reaction [30,72,77]. Different flowsheet layouts have been developed, with essentially two main configurations. The first approach sees the vacuum column product (i.e., concentrated H_2SO_4) pumped and fed directly to the high temperature decomposition unit with recirculation of the undecomposed sulfuric acid in the other sections of the plant [30]. The second approach sees the concentrated sulfuric acid pumped and fed to a quench column, where it contacts the effluent (recirculated, undecomposed sulfuric acid) from the decomposition reactor. The quench column is designed with a minimum number of equilibrium stages (e.g., two stages), one of which is the partial condenser [35,72]. The main advantage of the vacuum distillation concept resides in the relatively low operating temperatures, allowing effective internal heat recovery in the thermochemical plant and, therefore, resulting in increased process efficiencies. The main drawback is the low operating pressures (i.e., low volumetric flow rates), posing techno-economic challenges associated with the design of the components (distillation column, reboiler, condenser) that require large volumes [72,77].

The second acid concentration concept uses a series of flashes operating at pressures on the order of 1–10 bar and temperatures up to values on the order of 300–400 °C, depending on the required concentration level. Selected plant layouts and chemical flowsheets based on this approach can be found in References [13,42,44]. One configuration [13] proposes four pressure flash units, connected in series with a vacuum distillation column operating at 0.07 bar. The inlet sulfuric acid mixture, along with internally recycled sulfuric acid, is concentrated to 40 mole % in the high pressure four-stage isobaric concentrator operating at constant pressure of 35.5 bar and increasing temperatures from 299 °C up to 371 °C in the fourth flash unit [13]. The product of the isobaric concentration unit is concentrated in three flashes in series operating at 8 bar, 2 bar and 50 Torr before feeding the vacuum distillation unit. The bottom product of the distillation column is azeotropic sulfuric acid at approximately 90 mole % H_2SO_4 at 212°C [13]. Another flowsheet configuration [42,44] uses three pressure flash units, operating at different pressures and different temperatures. The sulfuric acid mixture feeds the three-stage concentrator at 57 wt %. The mixture is concentrated up to 87 wt % by the three-flash distillation process at different pressures (0.08 bar, 5.7 bar and 7 bar) reaching a final temperature (in the third flash) of 300 °C. The main drawback of the pressure multiple flash concentrator approach is the requirement of heating power at relatively high temperatures, provided either through internal heat recovery or an external source, resulting, in general, in a reduction in the overall cycle efficiency [13,42]. Lower sulfuric acid concentrations (i.e., on the order of 62.5 wt %) can be achieved at lower temperatures (144 °C) and lower pressures (1 bar), but this results in a reduced efficiency of the high temperature decomposition reactor [33].

3.3. Separation of Oxygen and Sulfur Dioxide

An important section in each sulfur based thermochemical process is relative to the O_2/SO_2 separation. Many approaches have been proposed lately to accomplish the SO_2/O_2 gas separation effectively [22,30,33,35]. One of the very few comprehensive SO_2/O_2 separation flowsheets available in the literature proposes the adoption of an O_2 stripper and an SO_2 stripper integrated with an SO_2 absorber and an oxygen dryer [35].

The SO_2 absorber, which separates oxygen from SO_2 based on the different water solubility, is an equilibrium column with multiple stages, without the presence of reboiler nor condenser. The chemical plant flowsheet includes an SO_2 absorber operating at a pressure of about 12 bar. The SO_2 feeding the absorber exits with the water in the bottoms of the units, almost entirely, while 99.7% of the oxygen exits with the overhead flow.

The SO_2 stripper, as proposed and simulated in Ref [35], has seven equilibrium stages operating at atmospheric pressure, including a partial vapor condenser and reboiler. SO_2 is stripped from the water solvent, allowing the water to be recycled and reused in the absorber.

The overhead from the SO_2 absorber contains less than 1 ppm SO_2, but it is saturated with water vapor at 11.8 bar and 40 °C [35]. It is passed through an O_2 dryer that removes the moisture, which is recycled in the plant. In the arrangement proposed in [35], pure oxygen is produced at 11 bar and 40 °C.

4. Conclusions

Sulfur based thermochemical processes are viable alternatives to electrolysis to produce hydrogen through water splitting. By using this approach, hydrogen can be produced without carbon-based emissions, with potential to achieve high efficiencies and low H_2 costs. These cycles can be coupled with either nuclear or solar plants, to produce hydrogen using a renewable source.

A review of the main sulfur processes was carried out and discussed. The Hybrid Sulfur process is likely the most advanced process, being able to be coupled with nuclear and solar power sources. The distinguishing section is comprised of an electrochemical system where sulfur dioxide is oxidized to produce sulfuric acid and hydrogen. Recent experimental tests demonstrated the ability of the electrochemical component, equipped with s-PBI membranes and Pt-based catalyst, to operate at 0.6–0.7 V and current densities of approximately 500 mA/cm^2. Realistic thermochemical cycle efficiencies on the order of 30–40% were documented in the literature, with H_2 production costs in the range of 2.64–7.58 $/kg. The Sulfur Iodine cycle is, in principle, a pure thermal process. The distinguishing section is the hydrogen iodide decomposition process. The cycle was extensively developed mainly for nuclear applications. Realistic thermochemical efficiencies on the order of 35–38% were reported, with high sensitivity to the adopted process configurations and approaches. Nuclear driven hydrogen production costs were estimated to be in the range of 3.50–12.0 $/kg. Another two sulfur-based processes were reviewed and compared, namely the Sulfur Bromine process and the Sulfur Ammonia process. The Sulfur Bromine cycle was extensively studied and developed at the end of 1970s for nuclear applications. The distinguishing section is the electrochemical decomposition of hydrobromic acid. The cycle was demonstrated experimentally for 100 L_{H2}/h. However, the high electric input required for the electrochemical reaction resulted in reduced interest in recent years. The Sulfur Ammonia process was developed by Florida Solar Energy Center for concentrated solar applications and represents an attempt to exploit both the thermal and the photonic components of the solar input. The cycle is more complicated than the other sulfur-based cycles, adding additional compounds and chemical sections. In addition, the cycle still requires fundamental research, both on thermodynamics and kinetics aspect, to achieve a prototype level demonstration.

Each sulfur-based thermochemical cycle sees the presence of a high temperature H_2SO_4 thermal section, where sulfuric acid is concentrated and decomposed, and oxygen is separated from the other compounds. Critical reviews were carried out for each process, analyzing and discussing the main process configurations and layouts proposed since the initial development. A specific review was carried out for the high temperature sulfuric acid decomposition section, discussing constitutive material options, catalytic formulations and decomposition reactor concepts. The referenced documents showed that ceramic materials (i.e., SiC materials) seem to be the most suitable option to withstand the high temperature aggressive environment. Currently, Pt-based catalysts represent the baseline formulation adopted to decompose sulfuric acid to sulfur dioxide, oxygen and water. Novel Pt-based bi-metallic formulations showed encouraging results, with preliminary tests highlighting high activity and minimal degradation. Metal oxide materials may have potential for high activity and high stability but still require additional fundamental work to avoid sintering and activity reduction at lower operating temperatures. Two main reactor concepts were discussed and compared. The first reactor, usually adopted for solar driven processes, is based on a direct cavity reactor concept, with the sulfuric acid decomposition occurring in two separate reactor units. The second concept, mostly employed in nuclear driven configurations, sees the presence of an intermediate heat transfer fluid exchanging the required thermal power. The indirect reactor concept seems to offer some advantages over the

direct cavity reactor, allowing the external heat transfer and the internal heat recovery to occur in a single unit.

Author Contributions: Conceptualization, C.C. and W.A.S.; methodology, C.C. and M.B.G.; resources, C.C.; writing—original draft preparation, C.C.; writing—review and editing, W.A.S. All authors have read and agreed to the published version of the manuscript.

Funding: This research received no external funding.

Acknowledgments: The authors wish to acknowledge Bunsen Wong (General Atomics), Daniel Ginosar (Idaho National Laboratory) and Martin Roeb (German Aerospace Center) for discussions during the manuscript conception and writing and for helping with the copyright permission of figures and tables included in the manuscript.

Conflicts of Interest: The authors declare no conflict of interest.

Nomenclature

HyS	Hybrid Sulfur
SI	Sulfur Iodine
SRNL	Savannah River National Laboratory
SNL	Sandia National Laboratory
PEM	Proton exchange membrane
LHV	Low heating value (120 MJ/kg_{H2})
DOE	U.S. Department of Energy
HFTO	DOE Hydrogen Fuel Cell Technology Office
DLR	German Aerospace Center
eNRTL	Electrolyte Non-Random Two Liquids
CFD	Computational Fluid Dynamic
s-PBI	Sulfonated polybenzimidazole

References

1. Pivovar, B.; Rustagi, N.; Satyapal, S. Hydrogen at Scale (H2@Scale): Key to a clean.; economic.; and sustainable energy system. *Electrochem. Soc. Interface* **2018**, *27*, 47–52. [CrossRef]
2. Perkins, C.; Weimer, A.W. Likely near-term solar-thermal water splitting technologies. *Int. J. Hydrogen Energy* **2004**, *29*, 1587–1599. [CrossRef]
3. Buttler, A.; Spliethoff, H. Current status of water electrolysis for energy storage.; grid balancing and sector coupling via power-to-gas and power-to-liquids: A review. *Renew. Sustain. Energy Rev.* **2018**, *82*, 2440–2454. [CrossRef]
4. Schmidt, O.; Gambhir, A.; Staffell, I.; Hawkes, A.; Nelson, J.; Few, S. Future cost and performance of water electrolysis: An expert elicitation study. *Int. J. Hydrogen Energy* **2017**, *42*, 30470–30492. [CrossRef]
5. Felgenhauer, M.; Hamacher, T. State-of-the-art of commercial electrolyzers and on-site hydrogen generation for logistic vehicles in South Carolina. *Int. J. Hydrogen Energy* **2015**, *40*, 2084–2090. [CrossRef]
6. Stoots, C.M.; O'Brien, J.E.; Condie, K.G.; Hartvigsen, J.J. High-temperature electrolysis for large-scale hydrogen production from nuclear energy–experimental investigations. *Int. J. Hydrogen Energy* **2010**, *35*, 4861–4870. [CrossRef]
7. Mougin, J. Hydrogen production by high-temperature steam electrolysis. In *Compendium of Hydrogen Energy*; Woodhead Publishing: Cambridge, UK, 2015; pp. 225–253.
8. Funk, J.E. Thermochemical hydrogen production: Past and present. *Int. J. Hydrogen Energy* **2001**, *26*, 185–190. [CrossRef]
9. Dincer, I.; Acar, C. Review and evaluation of hydrogen production methods for better sustainability. *Int. J. Hydrogen Energy* **2015**, *40*, 11094–11111. [CrossRef]
10. Steinfeld, A. Solar thermochemical production of hydrogen—-A review. *Solar. Energy* **2005**, *78*, 603–615. [CrossRef]
11. Beghi, G.E. A decade of research on thermochemical hydrogen at the joint research centre Ispra. *Int. J. Hydrogen Energy* **1986**, *11*, 761–771. [CrossRef]

12. Kodama, T.; Gokon, N. Thermochemical cycles for high-temperature solar hydrogen production. *Chem. Rev.* **2007**, *107*, 4048–4077. [CrossRef] [PubMed]
13. Brown, L.C.; Besenbruch, G.E.; Lentsch, R.D.; Schultz, K.R.; Funk, J.F.; Pickard, P.S.; Marshall, A.C.; Showalter, S.K. *High Efficiency Generation of Hydrogen Fuels Using Nuclear Power*; Final Technical Report from General Atomics Corp. to US DOE. GA-A24285; General Atomics: San Diego, CA, USA, 2003.
14. Abanades, S.; Charvin, P.; Flamant, G.; Neveu, P. Screening of water-splitting thermochemical cycles potentially attractive for hydrogen production by concentrated solar energy. *Energy* **2006**, *31*, 2805–2822. [CrossRef]
15. Russell, J.; Porter, J. *Production of Hydrogen from Water*; General Atomics Report GA–A12889; General Atomics: San Diego, CA, USA, 1974.
16. Norman, J.H.; Besenbruch, G.; O'keefe, D.R. *Thermochemical Water-Splitting for Hydrogen Production*; Final Report General Atomic Co PB-82-208174; General Atomics: San Diego, CA, USA, 1981.
17. Perret, R. *Solar Thermochemical Hydrogen Production Research (STCH)*; Sandia National Lab.(SNL-CA): Livermore, CA, USA, 2011. Available online: https://www1.eere.energy.gov/hydrogenandfuelcells/pdfs/solar_thermo_h2. (accessed on 24 September 2020).
18. Nuclear Hydrogen R&D Plan. DOE Fuel Cell Technology Office. 2004. Available online: https://www.energy.gov/sites/prod/files/2015/01/f19/fcto_nuclear_h2_r%26d_plan.pdf (accessed on 12 February 2019).
19. Yalcin, S. A review of nuclear hydrogen production. *Int. J. Hydrogen Energy* **1989**, *14*, 551–561. [CrossRef]
20. Brecher, L.E.; Spewock, S.; Warde, C.J. The westinghouse sulfur cycle for the thermochemical decomposition of water. *Int. J. Hydrogen Energy* **1977**, *2*, 7–15. [CrossRef]
21. Henderson, A.D.; Taylor, A. The US Department of Energy research and development programme on hydrogen production using nuclear energy. *Int. J. Nucl. Hydrog. Prod. Appl.* **2006**, *1*, 51–56. [CrossRef]
22. Corgnale, C.; Summers, W.A. Solar hydrogen production by the Hybrid Sulfur process. *Int. J. Hydrogen Energy* **2011**, *36*, 11604–11619. [CrossRef]
23. Elvington, M.C.; Colón-Mercado, H.; McCatty, S.; Stone, S.G.; Hobbs, D.T. Evaluation of proton-conducting membranes for use in a sulfur dioxide depolarized electrolyzer. *J. Power Sources* **2010**, *195*, 2823–2829. [CrossRef]
24. Staser, J.A.; Gorensek, M.B.; Weidner, J.W. Quantifying individual potential contributions of the hybrid sulfur electrolyzer. *J. Electrochem. Soc.* **2010**, *157*, B952–B958. [CrossRef]
25. Steimke, J.L.; Steeper, T.J.; Cólon-Mercado, H.R.; Gorensek, M.B. Development and testing of a PEM SO_2-depolarized electrolyzer and an operating method that prevents sulfur accumulation. *Int. J. Hydrogen Energy* **2015**, *40*, 13281–13294. [CrossRef]
26. Weidner, J.W. *High Performance Electrolyzers for Hybrid Thermochemical Cycles*; University of South Carolina Research Foundation (No. DOE/ID/14752); University of South Carolina: Columbia, SC, USA, 2009.
27. Garrick, T.R.; Wilkins, C.H.; Pingitore, A.T.; Mehlhoff, J.; Gulledge, A.; Benicewicz, B.C.; Weidner, J.W. Characterizing voltage losses in an SO_2 depolarized electrolyzer using sulfonated polybenzimidazole membranes. *J. Electrochem. Soc.* **2017**, *164*, F1591–F1595. [CrossRef]
28. Garrick, T.R.; Gulledge, A.; Staser, J.A.; Benicewicz, B.; Weidner, J.W. Polybenzimidazole membranes for hydrogen production in the hybrid sulfur electrolyzer. *ECS Trans.* **2015**, *66*, 31–40. [CrossRef]
29. Gorensek, M.B.; Corgnale, C.; Staser, J.A.; Weidner, J.W. Solar Thermochemical Hydrogen (STCH) Processes. *Electrochem. Soc. Interface* **2018**, *27*, 53–56. [CrossRef]
30. Gorensek, M.B.; Summers, W.A. Hybrid sulfur flowsheets using PEM electrolysis and a bayonet decomposition reactor. *Int. J. Hydrogen Energy* **2009**, *34*, 4097–4114. [CrossRef]
31. Colón-Mercado, H.R.; Hobbs, D.T. Catalyst evaluation for a sulfur dioxide-depolarized electrolyzer. *Electrochem. Commun.* **2007**, *9*, 2649–2653. [CrossRef]
32. Meekins, B.H.; Thompson, A.B.; Gopal, V.; Mehrabadi, B.A.; Elvington, M.C.; Ganesan, P.; Newhouse-lllige, T.A.; Shepard, A.W.; Scipioni, L.; Greer, J.A.; et al. In-situ and ex-situ comparison of the electrochemical oxidation of SO2 on carbon supported Pt and Au catalysts. *Int. J. Hydrogen Energy* **2020**, *45*, 1940–1947. [CrossRef]
33. Niehoff, A.G.; Botero, N.B.; Acharya, A.; Thomey, D.; Roeb, M.; Sattler, C.; Pitz-Paal, R. Process modelling and heat management of the solar hybrid sulfur cycle. *Int. J. Hydrogen Energy* **2015**, *40*, 4461–4473. [CrossRef]
34. Corgnale, C.; Gorensek, M.; Summers, W.A. *Solar Hybrid Sulfur Cycle Water-Splitting Process*; SRNL-STI-2015e00546; Revision 0; Savannah River National Laboratory: Aiken, SC, USA, 2015.

35. Gorensek, M.B.; Corgnale, C.; Summers, W.A. Development of the hybrid sulfur cycle for use with concentrated solar heat. I. Conceptual design. *Int. J. Hydrogen Energy* **2017**, *42*, 20939–20954. [CrossRef]
36. Gorensek, M.; Summers, W.; Boltrunis, C.; Lahoda, E.; Allen, D.; Greyvenstein, R. *Hybrid Sulfur Process Reference Design and Cost Analysis*; Report No. SRNL-L1200-2008-00002; Savannah River National Laboratory: Aiken, SC, USA, 2009.
37. Summers, W.A.; Buckner, M.R.; Gorensek, M.B. The hybrid sulfur cycle for nuclear hydrogen production. In Proceedings of the GLOBAL 2005, Tsukuba, Japan, 9–13 October 2005.
38. Hinkley, J.T.; O'Brien, J.A.; Fell, C.J.; Lindquist, S.E. Prospects for solar only operation of the hybrid sulphur cycle for hydrogen production. *Int. J. Hydrogen Energy* **2011**, *36*, 11596–11603. [CrossRef]
39. Kromer, M.; Roth, K.; Takata, R.; Chin, P. Support for Cost Analyses on Solar-Driven High Temperature Thermochemical Water-Splitting Cycles. Final Report to DOE DE-DT0000951. 2011. Available online: https://www.energy.gov/sites/prod/files/2014/03/f11/solar_thermo_h2_cost.pdf (accessed on 23 September 2020).
40. U.S. Department of Energy HydroGEN Program. Available online: https://www.h2awsm.org/ (accessed on 8 August 2020).
41. O'keefe, D.; Allen, C.; Besenbruch, G.; Brown, L.; Norman, J.; Sharp, R.; McCorkle, K. Preliminary results from bench-scale testing of a sulfur-iodine thermochemical water-splitting cycle. *Int. J. Hydrogen Energy* **1982**, *7*, 381–392. [CrossRef]
42. Cerri, G.; Salvini, C.; Corgnale, C.; Giovannelli, A.; Manzano, D.D.L.; Martinez, A.O.; le Duigou, A.; Borgard, J.-M.; Mansilla, C. Sulfur–Iodine plant for large scale hydrogen production by nuclear power. *Int. J. Hydrogen Energy* **2010**, *35*, 4002–4014. [CrossRef]
43. International Atomic Energy Agency. *Hydrogen Production Using Nuclear Energy*; IAEA Nuclear Energy Series No. NP-T-4.2; International Atomic Energy Agency: Vienna, Austria, 2013.
44. LeDuigou, A.; Borgard, J.M.; Larousse, B.; Doizi, D.; Allen, R.; Ewan, B.C.; Priestman, G.H.; Elder, R.; Devonshire, R.; Ramos, V.; et al. HYTHEC: An EC funded search for a long term massive hydrogen production route using solar and nuclear technologies. *Int. J. Hydrogen Energy* **2007**, *32*, 1517–1529.
45. Onuki, K.; Kubo, S.; Terada, A.; Sakaba, N.; Hino, R. Thermochemical water-splitting cycle using iodine and sulfur. *Energy Environ. Sci.* **2009**, *2*, 491–497. [CrossRef]
46. Mysels, K.J. Method of Extracting Iodine from Liquid Mixtures of Iodine, Water and Hydrogen Iodide. U.S. Patent 4176169, 27 November 1979.
47. Cho, W.C.; Park, C.S.; Kang, K.S.; Kim, C.H.; Bae, K.K. Conceptual design of sulfur–iodine hydrogen production cycle of Korea Institute of Energy Research. *Nucl. Eng. Des.* **2009**, *239*, 501–507. [CrossRef]
48. Guo, H.; Kasahara, S.; Tanaka, N.; Onuki, K. Energy requirement of HI separation from HI–I_2–H_2O mixture using electro-electrodialysis and distillation. *Int. J. Hydrogen Energy* **2012**, *37*, 13971–13982. [CrossRef]
49. Berndhaeuser, C.; Knoche, K.F. Experimental investigations of thermal HI decomposition from H2O-HIx-I2 solutions. *Int. J. Hydrogen Energy* **1994**, *19*, 239–244. [CrossRef]
50. Murphy, J.E., IV; O'Connell, J.P. Process simulations of HI decomposition via reactive distillation in the sulfur–iodine cycle for hydrogen manufacture. *Int. J. Hydrogen Energy* **2012**, *37*, 4002–4011. [CrossRef]
51. Norman, J.H.; Mysels, K.J.; Sharp, R.; Williamson, D. Studies of the sulfur-iodine thermochemical water-splitting cycle. *Int. J. Hydrogen Energy* **1982**, *7*, 545–556. [CrossRef]
52. Leybros, J.; Gilardi, T.; Saturnin, A.; Mansilla, C.; Carles, P. Plant sizing and evaluation of hydrogen production costs from advanced processes coupled to a nuclear heat source. Part I: Sulphur–iodine cycle. *Int. J. Hydrogen Energy* **2010**, *35*, 1008–1018. [CrossRef]
53. van Velzen, D.; Langenkamp, H.; Schutz, G.; Lalonde, D.; Flamm, J.; Fiebelmann, P. Development and design of a continuous laboratory scale plant for hydrogen production by the Mark-13 cycle. *Int. J. Hydrogen Energy* **1980**, *5*, 131–139. [CrossRef]
54. van Velzen, D.; Langenkamp, H. Status report on the operation of the bench-scale plant for hydrogen production by the mark-13 process. *Int. J. Hydrogen Energy* **1982**, *7*, 629–636. [CrossRef]
55. T-Raissi, A.; Muradov, N.; Huang, C.; Adebiyi, O. Hydrogen from solar via light-assisted high-temperature water splitting cycles. *J. Solar. Energy Eng.* **2007**, *129*, 184–189. [CrossRef]
56. Kalyva, A.E.; Vagia, E.C.; Konstandopoulos, A.G.; Srinivasa, A.R.; T-Raissi, A.; Muradov, N.; Kakosimos, K.E. Investigation of the solar hybrid photo-thermochemical sulfur-ammonia water splitting cycle for hydrogen production. *Chem. Eng. Trans.* **2015**, *45*, 361–366.

57. Littlefield, J.; Wang, M.; Brown, L.C.; Herz, R.K.; Talbot, J.B. Process modeling and thermochemical experimental analysis of a solar sulfur ammonia hydrogen production cycle. *Energy Procedia* **2012**, *29*, 616–623. [CrossRef]
58. Kaur, H.; Wang, M.; Gorensek, M.B.; Chen, C.C. Thermodynamic modeling of the hybrid sulfur (HyS) cycle for hydrogen production. *Fluid Phase Equilibria* **2018**, *460*, 175–188. [CrossRef]
59. Wong, B.; Trester, P.W. *Materials Development for Sulfur-Iodine Thermochemical Hydrogen*; General Atomics Report GA-A25750; General Atomics: San Diego, CA, USA, 2007; Chapter 4.
60. Wong, B.; Buckingham, R.T.; Brown, L.C.; Russ, B.E.; Besenbruch, G.E.; Kaiparambil, A.; Roy, A. Construction materials development in sulfur–iodine thermochemical water-splitting process for hydrogen production. *Int. J. Hydrogen Energy* **2007**, *32*, 497–504. [CrossRef]
61. Kubo, S.; Futakawa, M.; Ioka, I.; Onuki, K.; Yamaguchi, A. Corrosion resistance of structural materials in high-temperature aqueous sulfuric acids in thermochemical water-splitting iodine–sulfur process. *Int. J. Hydrogen Energy* **2013**, *38*, 6577–6585. [CrossRef]
62. Karagiannakis, G.; Agrafiotis, C.C.; Pagkoura, C.; Konstandopoulos, A.G.; Thomey, D.; de Oliveira, L.; Roeb, M.; Sattler, C. Hydrogen production via sulfur-based thermochemical cycles: Part 3: Durability and post-characterization of silicon carbide honeycomb substrates coated with metal oxide-based candidate catalysts for the sulfuric acid decomposition step. *Int. J. Hydrogen Energy* **2012**, *37*, 8190–8203. [CrossRef]
63. Roeb, M.; Neises, M.; Monnerie, N.; Call, F.; Simon, H.; Sattler, C.; Schmücker, M.; Pitz-Paal, R. Materials-related aspects of thermochemical water and carbon dioxide splitting: A review. *Materials* **2012**, *5*, 2015–2054. [CrossRef]
64. O'keefe, D.R.; Norman, J.H.; Williamson, D.G. Catalysis research in thermochemical water-splitting processes. *Catal. Rev. Sci. Eng.* **1980**, *22*, 325–369. [CrossRef]
65. Tagawa, H.; Endo, T. Catalytic decomposition of sulfuric acid using metal oxides as the oxygen generating reaction in thermochemical water splitting process. *Int. J. Hydrogen Energy* **1989**, *14*, 11–17. [CrossRef]
66. Schultz, K.; Sink, C.; Pickard, P.; Herring, S.; O'Brien, J.; Buckingham, B.; Summers, W.; Lewis, M. Status of the US nuclear hydrogen initiative. In Proceedings of the ICAPP Conference, Bangkok, Thailand, 20–25 June 2007. Paper 7530:13-8.
67. Ginosar, D.M.; Petkovic, L.M.; Glenn, A.W.; Burch, K.C. Stability of supported platinum sulfuric acid decomposition catalysts for use in thermochemical water splitting cycles. *Int. J Hydrogen Energy* **2007**, *32*, 482–488. [CrossRef]
68. Petkovic, L.M.; Ginosar, D.M.; Rollins, H.W.; Burch, K.C.; Pinhero, P.J.; Farrell, H.H. Pt/TiO_2 (rutile) catalysts for sulfuric acid decomposition in sulfur-based thermochemical water-splitting cycles. *Appl. Catal. A Gen.* **2008**, *338*, 27–36. [CrossRef]
69. Ginosar, D.M.; Rollins, H.W.; Petkovic, L.M.; Burch, K.C.; Rush, M.J. High-temperature sulfuric acid decomposition over complex metal oxide catalysts. *Int. J. Hydrogen Energy* **2009**, *34*, 4065–4073. [CrossRef]
70. Karagiannakis, G.; Agrafiotis, C.C.; Zygogianni, A.; Pagkoura, C.; Konstandopoulos, A.G. Hydrogen production via sulfur-based thermochemical cycles: Part 1: Synthesis and evaluation of metal oxide-based candidate catalyst powders for the sulfuric acid decomposition step. *Int. J. Hydrogen Energy* **2011**, *36*, 2831–2844. [CrossRef]
71. Giaconia, A.; Sau, S.; Felici, C.; Tarquini, P.; Karagiannakis, G.; Pagkoura, C.; Agrafiotis, C.; Konstandopoulos, A.G.; Thomey, D.; de Oliveira, L.; et al. Hydrogen production via sulfur-based thermochemical cycles: Part 2: Performance evaluation of Fe2O3-based catalysts for the sulfuric acid decomposition step. *Int. J. Hydrogen Energy* **2011**, *36*, 6496–6509. [CrossRef]
72. Corgnale, C. High temperature reactor catalyst material development for low cost and efficient solar driven sulfur-based processes. In Proceedings of the DOE Annual Merit Review Presentation, Crystal City, VV, USA, 19–21 May 2019.
73. Noglik, A.; Roeb, M.; Rzepczyk, T.; Hinkley, J.; Sattler, C.; Pitz-Paal, R. Solar thermochemical generation of hydrogen: Development of a receiver reactor for the decomposition of sulfuric acid. *J. Solar. Energy Eng.* **2009**, *131*, 011003-1. [CrossRef]
74. Thomey, D.; de Oliveira, L.; Sack, J.-P.; Roeb, M.; Sattler, C. Development and test of a solar reactor for decomposition of sulphuric acid in thermochemical hydrogen production. *Int. J. Hydrogen Energy* **2012**, *37*, 16615–16622. [CrossRef]

75. Moore, R.; Pickard, P.; Parma, E.; Vernon, M.; Gelbard, F. Integrated Boiler.; Superheater and Decomposer for Sulphuric Acid Decomposition. Sandia Corp. U.S. Patent No. 7645437 B1, 12 January 2010.
76. Russ, B. Sulfur Iodine Process Summary for the Hydrogen Technology Down-Selection. Available online: https://art.inl.gov/NGNP/Subcontractors%20Documents/General%20Atomics/Sulfur%20Iodine%20Process%20Summary%20for%20the%20Hydrogen%20Technology%20Down-Selection.pdf (accessed on 20 September 2020).
77. Sattler, C.; Roeb, M.; Agrafiotis, C.; Thomey, D. Solar hydrogen production via sulphur based thermochemical water-splitting. *Solar Energy* **2017**, *156*, 30–47. [CrossRef]
78. Gorensek, M.B.; Edwards, T.B. Energy efficiency limits for a recuperative bayonet sulfuric acid decomposition reactor for sulfur cycle thermochemical hydrogen production. *Ind. Eng. Chem. Res.* **2009**, *48*, 7232–7245. [CrossRef]
79. Corgnale, C.; Shimpalee, S.; Gorensek, M.; Satjaritanun, P.; Weidner, J.; Summers, W. Numerical modeling of a bayonet heat exchanger-based reactor for sulfuric acid decomposition in thermochemical hydrogen production processes. *Int. J. Hydrogen Energy* **2017**, *42*, 2046. [CrossRef]
80. Corgnale, C.; Ma, Z.; Shimpalee, S. Modeling of a direct solar receiver reactor for decomposition of sulfuric acid in thermochemical hydrogen production cycles. *Int. J. Hydrogen Energy* **2019**, *44*, 27237–27247. [CrossRef]